EurJOC
European Journal of Organic Chemistry

Research Article
doi.org/10.1002/ejoc.202200372

Chemistry Europe
European Chemical Societies Publishing

www.eurjoc.org

Special Collection

Asymmetric Dual-State Emitters Featuring Thiazole Acceptors

José L. Belmonte-Vázquez,*[a] Ernesto A. Hernández-Morales,[a] Federico. Hernández,[b] Ma. Carmen García-González,[a] Luis D. Miranda,[a] Rachel Crespo-Otero,[b] and Braulio Rodríguez-Molina*[a]

This work describes a new approach to construct highly conjugated molecules with asymmetric donor-acceptor-donor' architectures (D–A–D'). Five new emissive compounds featuring thiazole, a scarcely used acceptor, were synthesized using a three-component Rh(II) catalytic reaction. The asymmetric fluorescent compounds show significant emission in solution (QY = 73 %–100 %) and the solid-state (QY = 14 %–59 %), and therefore considered Dual-State Emitters (DSE). We also evaluate the impact of O-alkyl chains with varying lengths in the photophysical properties in solution, aggregates, and solid-state. Computational studies indicate that the involved electronic transitions have a significant charge transfer character produced almost exclusively from the triphenylamine donors. According to the single crystal X-ray data of compounds **8** and **9**, the conjugated structures have a twisted molecular conformation that contributes to the observed emission in the solid-state. These findings show a systematic approach to design DSE materials, which may help to stimulate their use in biological or optoelectronic applications.

Introduction

The synthesis of organic fluorophores with emission in solution and in solid-state (Dual-State Emission - DSE) has recently attracted a great deal of interest, in part due to the plethora of potential applications.[1] Several research groups have turned their focus to design, and evaluate these exciting materials that can be used as biological probes or components in optoelectronic devices.[2] The development of DSE fluorophores (DSEgens) is still challenging because it relies on a delicate balance between two mutually exclusive processes, in which the fluorescent molecules experience loss of their emission in the solid-state (Aggregation Caused Quenching-ACQ) or in solution (Solid-state Luminescence Enhancement-SLE or Aggregation-Induced Emission-AIE), respectively.[3]

We and others, have recently surveyed the literature and pointed out that some specific characteristics of a molecule to enable the desired dual-state emissive properties, *i.e.*, a) twisted conjugated structures, b) restricted intramolecular motion, and c) the inclusion of bulky or long alkyl chains.[4] These guidelines should be kept in mind when designing new DSEgens, as it would be interesting to systematically explore the degree of twisting or the length of aliphatic chains that render the best properties in a specific set of compounds.

In addition to the mentioned structural features, it has been reported that several fluorophores and some DSEgens have Donor-Acceptor (D–A) or Donor-Acceptor-Donor (D–A–D) architectures.[5–7] This is a recurring design that helps to change the emission of the compounds by tuning their bandgap.[8] From the numerous reported D–A and D–A–D compounds, we noted that the heterocycle thiazole has been scarcely incorporated as the acceptor fragment, compared to other heterocycles like benzothiadiazole. Remarkable examples can be found in the reports of Huang,[9] Belskaya,[10] Murai,[11] and Nallagondu,[12] in which they have explored thiazoles with different substituents, substitution patterns, and varying length of the conjugated fluorophore skeleton, with the resulting emission ranging from 390 nm to 726 nm.[9,13] Some of these thiazole derivatives have been used in WOLEDs,[14] solar cells,[15] OFETs, and OPVs.[16] It is also important to mention that most synthetic methods afford either 2,4,5-trisubstituted[10,17] or 2,4-disubstituted thiazoles,[18] and that fluorophores with 2,5-disubstituted thiazoles are very scarce, with some notable examples reported as DSEgens.[9,19]

In this work, we present the design and synthesis of a new series of fluorophores **7**–**11** featuring a thiazole acceptor as well as the study of their corresponding photophysical properties in solution and in the solid-state. We consider a D–A–D' architecture with one carbazole moiety as a constant donor

[a] Dr. J. L. Belmonte-Vázquez, BSc. E. A. Hernández-Morales, Dr. M. C. García-González, Dr. L. D. Miranda, Dr. B. Rodríguez-Molina
Instituto de Química
Universidad Nacional Autónoma de México
Circuito Exterior, Ciudad Universitaria, 04510, Ciudad de México, México
E-mail: jl.belmontevazquez@iquimica.unam.mx
brodriguez@iquimica.unam.mx
[b] Dr. F. Hernández, Dr. R. Crespo-Otero
Department of Chemistry
Queen Mary University
London, UK

Supporting information for this article is available on the WWW under https://doi.org/10.1002/ejoc.202200372

Part of the "Organic and Supramolecular Chemistry in Latin America" Special Collection.

Research Article
doi.org/10.1002/ejoc.202200372

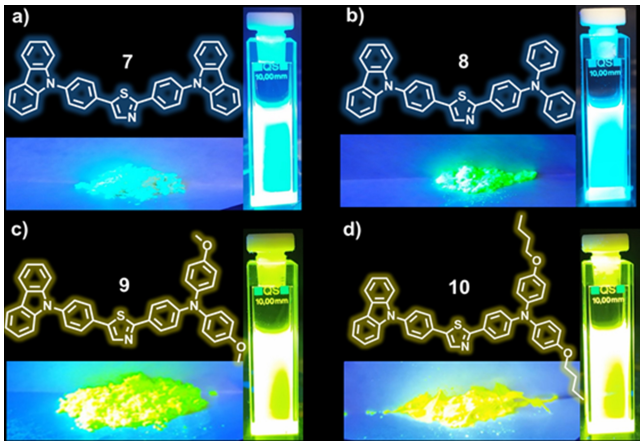

Figure 1. Selected structures of 2,5-disubstituted thiazole D–A–D′ fluorophores with Dual-State Emission reported here. Compound **11** is not depicted because it is a waxy solid.

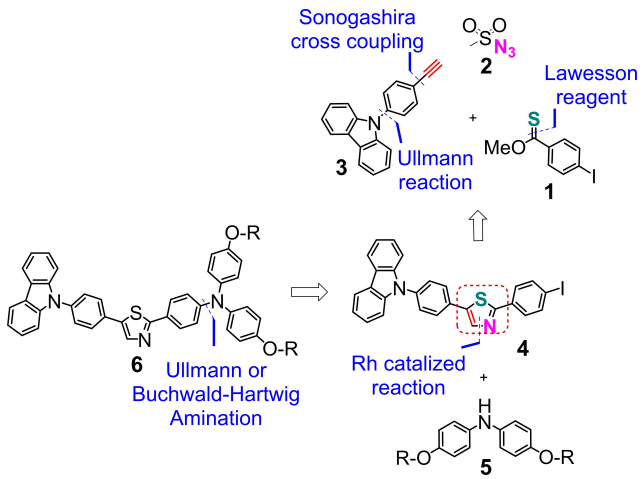

Scheme 1. Retrosynthetic analysis of the D–A–D′ products reported in this work.

fragment, a thiazole unit as the acceptor, and either carbazole or TPA derivatives as the second donor (Figure 1 and S1).

The synthesized D–A–D′ compounds were purposely appended with alkyl chains of varying length in the periphery of their structures, to explore if their photophysical properties can be further modified. As indicated above, these aliphatic substituents usually help to achieve DSE properties by promoting the self-isolation effect,[20] preventing undesirable π-π intermolecular interactions and thus avoiding the aggregation-caused quenching. This inner dilution strategy causes a somehow similar effect to that occurring when dispersing fused fluorophores in polymers such as polystyrene (PS) or polymethylmethacrylate (PMMA).[21]

Results and Discussion

Our synthetic strategy relies on the synthesis of parent derivative **4**, which contains the thiazole ring with the desired substitution pattern (Scheme 1). Although there are methods to synthesize 2,5-disubstituted thiazoles, either through sequential cross coupling reactions or programmed C–H activations over the thiazole core,[22] the one-pot generation of the thiazole moiety for complex dyes usually occurs with very low yields and gives rise to side products with different substitution patterns.[9,23] Thus, we took advantage of a Rh(II)-catalyzed three-component reaction between an alkyne, a thionoester and several azide derivatives, to prepare exclusively an intermediary with a 2,5-disubstituted thiazole.

The key three-component reaction was reported by Murakami *et al.* although this approach was not used to prepare fluorophores.[24] We envisioned that the Murakami protocol might produce new D–A–D′ thiazole-based molecules with extended conjugation. Therefore, we carry out a retrosynthetic analysis, where we envisioned that the analogues of **6** (Scheme 1) could be obtained by employing an Ullmann-type coupling or Buchwald-Hartwig amination reaction, between the intermediate **4** and the appropriate diphenylamine derivative **5**. The derivative **4** could in turn be prepared by using the rhodium-catalyzed reaction (highlighted by the red dotted line) using the simple starting materials **1**–**3**. In parallel, the intermediate **5** could be synthesized in a two-step sequence of bromination of diphenylamine followed by a nucleophilic aromatic substitution to install the aliphatic chains.

As our approach relied on the one-pot synthesis of 2,5-disubstituted extended thiazoles, we first synthesized the terminal alkyne **3**[25] and the *O*-methyl 4-iodobenzothioate **1**,[26] to access compound **4** with a moderate yield of 65% (Scheme 2).

Subsequently, the target compound **7** was prepared using an Ullmann type reaction with 37% yield. The C–N coupling reaction conditions did not produce the desired TPA derivatives, and thus we explored a few Buchwald-Hartwig reaction variations as indicated in Table S1 (SI). The best reaction conditions are in entry 4, producing the desired product **8** with a yield of 28%. We employed these conditions to obtain the additional derivatives **9**–**11** with better yields (37%–50%). The latter compounds have aliphatic chains of different lengths (Figure 2) to explore the self-isolation effect, as discussed in the introduction.

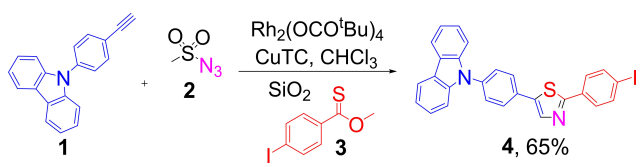

Scheme 2. Synthesis of compound **4** under a Rhodium-catalyzed three-component reaction.

Research Article
doi.org/10.1002/ejoc.202200372

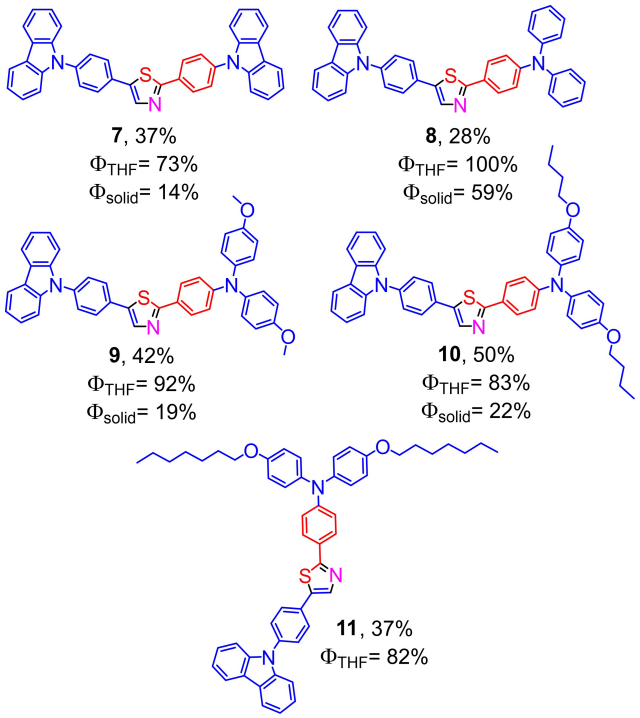

Figure 2. Chemical structures of the D–A–D′ fluorophores with 2,5-disubstituted thiazoles reported here with the reaction (%) and quantum yields (Φ) in solution and in the solid-state.

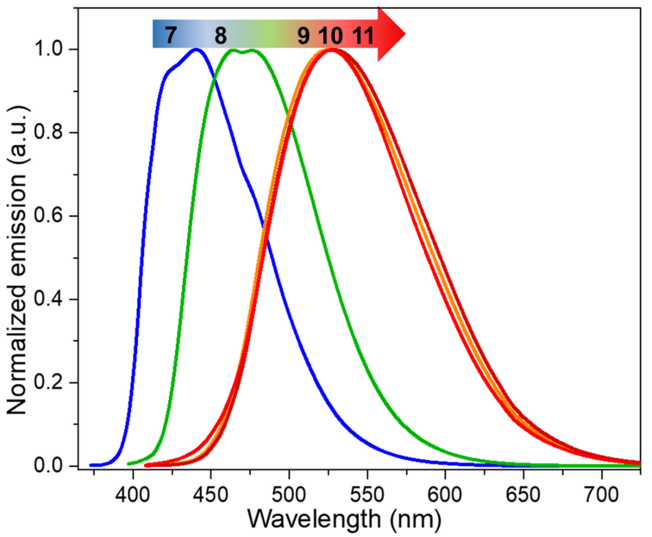

Figure 3. Fluorescence of the thiazole-based derivatives **7**–**11** in THF solution [4×10^{-3} M].

Table 1. Photophysical data of compounds **7**–**11**.

Compound	λ_{abs} [nm][a]	λ_{em} [nm][a] solution	Stokes shift [nm/cm^{-1}]	λ_{em} [nm] solid	Φ_{THF}[b]/Φ_{Solid}[b] [%]
7	365	440	75/4670	471	73/14
8	388	464	76/4220	502	100/59
9	397	525	128/6141	533	92/18
10	400	528	128/6061	526	83/22
11	399	526	127/6051	N.D	82/N.D

[a] Measured in THF [4×10^{-3} M]. [b] Absolute quantum yields. N.D: Not determined.

Photophysical properties

Changes in emission due to polarity of the media

After completing the synthesis of the fluorophores, we carried out spectroscopic experiments of compounds **7**–**11** to characterize their photophysical properties. The absorption and emission profiles ($\lambda_{abs}/\lambda_{em}$) were recorded first in THF to carry out an initial comparison. The inspection of the emission spectra reveals that replacing one carbazole portion (compound **7**, $\lambda_{em}=440$ nm) by diphenylamine (compound **8**, $\lambda_{em}=464$ nm) produced a 24 nm bathochromic red-shift of the initial emission.

Our studies also corroborate that the aliphatic substituents (*O*-Methyl **9**, *O*-Butyl **10**, and *O*-Heptyl **11**) strengthen the donor nature of the triphenylamine portion, with all alkyl-substituted derivatives **9**–**11**, showing a larger red-shift in the emission (61 nm) (Figure 3). A notable quantum yield in solution was observed for compound **8** ($\Phi_{THF}=100\%$). It is important to note that the QY slightly decreases as the size of the alkyl chains increases: **9** (*O*-Methyl; $\Phi_{THF}=92\%$), **10** (*O*-Butyl: $\Phi_{THF}=83\%$), and **11** (*O*-Heptyl; $\Phi_{THF}=82\%$). The QY reduction could come from the additional molecular mobility of the aliphatic substituents that could transfer to the donor portion. However, in general, the presence of the peripheral chains improved the emission, as can be seen by analyzing the emission of compound **7** ($\Phi_{THF}=73\%$, Table 1).

After we established the emission in THF, we performed a systematic study in thirteen different organic solvents of different polarities at room temperature (Figures S2–S3, S10, and Table S2). Despite that thiazole has been considered a 'weak' acceptor,[27] pairing this core with the selected carbazole or triphenylamine donors renders good D–A–D′ compounds. The changes in emission show that fast reorientations of the molecules take place in the excited state, with the larger response observed in polar media for compounds **9**, **10**, and **11** (Figure 4), resulting from stronger donors due to the *O*-alkyl substituents.

Computational modelling

To get a deeper understanding of the photophysical properties presented in the previous section, we have modelled the electronic transitions to the first bright state S_1 with the method TD-CAM-B3LYP/6-311++G** and considering two solvents to represent media of small and large dielectric constant (cyclohexane, $\varepsilon=2.02$, and methanol, $\varepsilon=32.61$, SI). The absorption wavelengths agree very well with the experimental values (see Table S2). For all molecules, the electronic transition $S_0\rightarrow S_1$ is a HOMO-LUMO π-π^* with charge transfer (CT) character. The electron density is transferred from the external

Research Article
doi.org/10.1002/ejoc.202200372

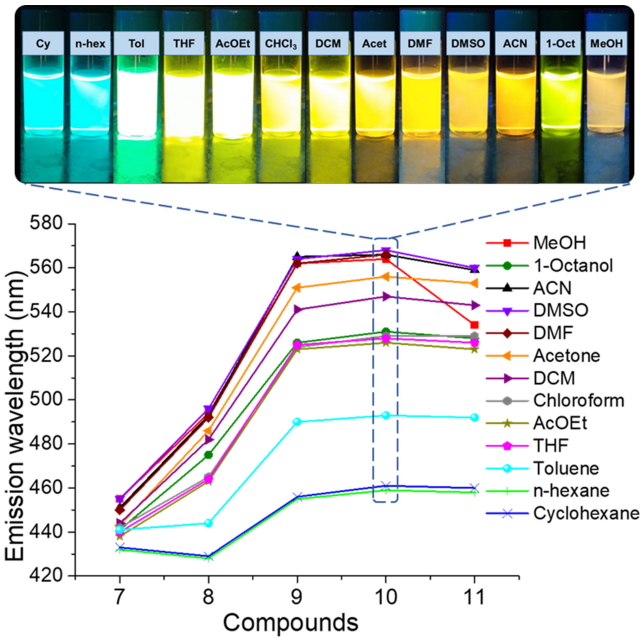

Figure 4. Plot of compounds **7**–**11** against their emission maxima, in solvents of different polarities. Insert: Changes of compound **10** are visible to the naked eye.

donors to the central part of the molecule as indicated by the HOMO-LUMO separation (see Figure 5a, S7 and S8).

Vibrational cooling, occurring after light absorption, drives the system from the Franck-Condon region to the minimum in S_1 (S_{1min}). This process involves angular displacements between the thiazole and the two central benzene rings adopting a planar conformation, with the additional motion of the D′ moiety (Figure 5b and S9). This significant structural change justifies the big Stokes shifts observed experimentally and supported by our calculations (Table S2). These molecular distortions are in line with the obtained crystalline structures (*vide infra*). The predicted $S_1 \rightarrow S_0$ fluorescence wavelengths in cyclohexane and methanol also agree with the experimental values (Table S2). Additionally, the general trend observed for the changes in emission with the media polarity is also reproduced by the calculations (Figure 4 and Figure 6a.

The increase in the bathochromic shifts observed when going from **7** to **11** corroborates that the electron-donating nature of this portion is strengthened when one carbazole is replaced by triphenylamine, and then again when this amine is substituted with *O*-aliphatic chains (Figure 3). Likewise, the bathochromic shifts increase with dielectric constant of the solvent (Figure 4). Compound **7** shows the smallest CT whereas compounds **9**–**11** exhibit the greatest CT. We have also calculated the changes in the permanent electric dipole moment $\Delta\mu_{S1\text{-}S0}$ (Figure 6b). Because of the significant charge separation, CT transitions are accompanied by a noticeable $\Delta\mu$. In line with the behavior observed for the charges, the $\Delta\mu$ is smaller for **7** ($\Delta\mu \approx 0.5$ Debye), considerably larger for **8** ($\Delta\mu \approx 4.0$–5.5 Debye), and even larger for **9**–**11** ($\Delta\mu \approx 8.0$–8.8 Debye). Besides, $\Delta\mu$ values are slightly larger for compounds **8**–**11** by changing the dielectric constant from 2.02 (cyclohexane) to 32.61 (methanol), as expected for CT transitions (Figure 6b).

The differences between the natural charges at S_1 and S_0 ($\Delta qS_1\text{-}S_0$) show a significant charge migration due to the electronic excitation (Figure 6c and Figure 6d). Except for compound **7**, for which D = D′, charge donation occurs almost exclusively from D′ to A. The derivatization of the triphenylamine by including *O*-alkyl chains has a positive effect on its donation strength. However, the natural charge analysis shows that longer chains do not increase the donation strength, in line with the similar redshifts observed for **9**–**11** (Figure 3 and Figure 4). As expected, the charge donation becomes more significant when the polarity of the media is increased.

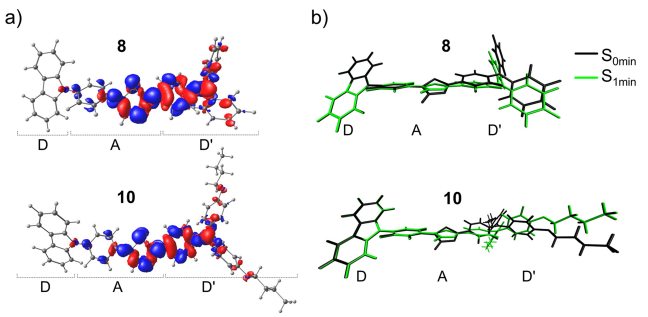

Figure 5. (a) Electron density difference of the transition $S_0 \rightarrow S_1$ for compounds **8** and **10** calculated with TD-CAM-B3LYP/6-311++G(d,p) considering methanol as a solvent. The positive and negative densities are shown in red and blue, respectively. (b) Optimized geometries of **8** and **10** at S_0 (S_{0min}) and S_1 (S_{1min}) states.

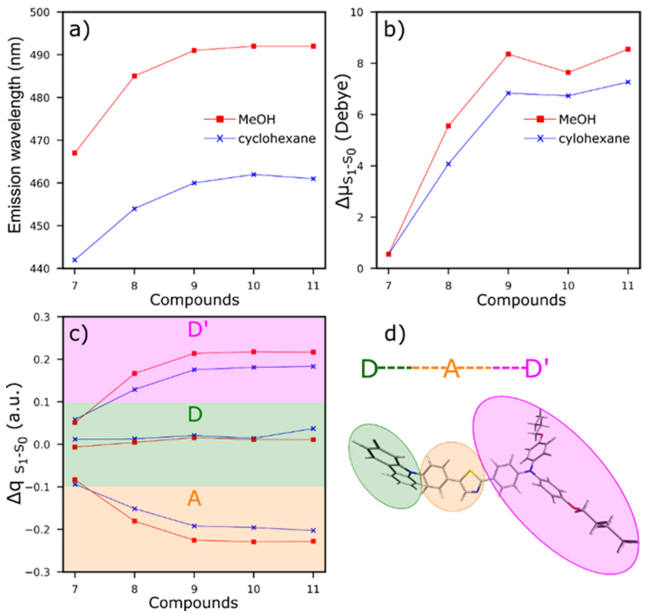

Figure 6. $S_1 \rightarrow S_0$ emission wavelengths (a), permanent electric dipole moment differences $\Delta\mu_{S1\text{-}S0}$ (b) and natural charge differences $\Delta\mu_{S1\text{-}S0}$ (c) computed with TD-CAM-B3LYP/6-311++G(d,p) in cyclohexane and methanol (blue and red lines respectively). (d) Definition of the donors (D and D′) and the acceptor (A) fragments for compound 10.

Research Article
doi.org/10.1002/ejoc.202200372

Evaluation of the intramolecular motion by viscosity changes

The fluorescence changes and the theoretical results motivated us to explore how the molecular reorientations could be changed in high viscosity media. For a more direct comparison, we present here the results for compounds **8** (unsubstituted donor D′), and **10** (donor D′ with –*O*Butyl groups), measuring their emission in different mixtures of methanol-glycerol (MeOH/GlyOH), a system known to dramatically increase the viscosity with small variations in the polarity.

For compound **8**, the initial emission showed a substantial decrease at viscosities higher than $f_{gly}=40\,\%$ (Figure 7a, Figure 7b). Conversely, we observed a ten-fold increase in the emission intensity of compound **10** at higher viscosity conditions. This suggests that the triphenylamine with the aliphatic chains experiences a high degree of mobility in pure MeOH. These vibrations are subsequently restricted at high glycerol content, reaching a maximum intensity at $f_{gly}=70\,\%$ (Figure 7c, Figure 7d). The observed changes in emission are in line with the Restricted Intramolecular Motion model (RIM).[28] Afterwards, the emission decreases probably due to scattering effects. Compound **9** showed a similar behavior, reaching its higher emission intensity at $f_{gly}=90\,\%$ (Figure S6).

Aggregation behavior and self-isolation effect in compounds 7–11

Aggregation-induced emission (AIE) experiments were subsequently performed to elucidate which compounds can form highly emissive aggregates. These experiments also helped us evaluate the role of the peripheral aliphatic chains in the self-isolation effect. Based on previous reports,[5,29] this effect occurs when the long or bulky substituents minimize the deleterious intermolecular π-π interactions that arise upon aggregation and may cause fluorescence quenching. The emission of the fluorophores is monitored as a function of the water fraction f_w in a THF solution.

Our studies indicate that compound **7** showed a steady emission intensity up to $f_w=50\,\%$, with a drastic loss of intensity at or above $f_w=60\,\%$. Similarly, compound **8**, in which the second donor does not have aliphatic substituents, also presented an ACQ behavior, with emission quenching with the addition of water fractions (Figure 8b). Compound **9** with the -OMe substituents showed a slightly different behavior, with the emission being reduced at low water contents ($f_w<70\,\%$), but then increased above $f_w=80\,\%$. Nevertheless, the observed intensity is still lower than that observed in pure THF, and higher water fractions cause a significant loss of fluorescence.

In stark contrast, compounds **10** and **11**, both with longer aliphatic chains attached to their structures, showed a remarkable increase in emission at $f_w=60\,\%$ and above, with an intensity comparable to that in pure THF (Figure 8d, Figure 8e, Figure 8f, and Figure S4). These results indicate that the chains of four (compound **10**) and seven carbon atoms (compound **11**) might enable the creation of highly emissive aggregates, attributed to the presence of the self-isolation effect in these compounds.[20a]

To provide deeper insights, we carried out a detailed comparison of the I/I_0 ratio between compounds **8** and **10** (Figure S5). The emission intensity (I_0) of compound **8** continuously decreases at high water fractions, associated to deleterious interactions. Conversely, the initial decrease in emission intensity for compound **10**, between $f_w=10\,\%$ and 60 %, could be attributed to the changes in polarity caused by water.

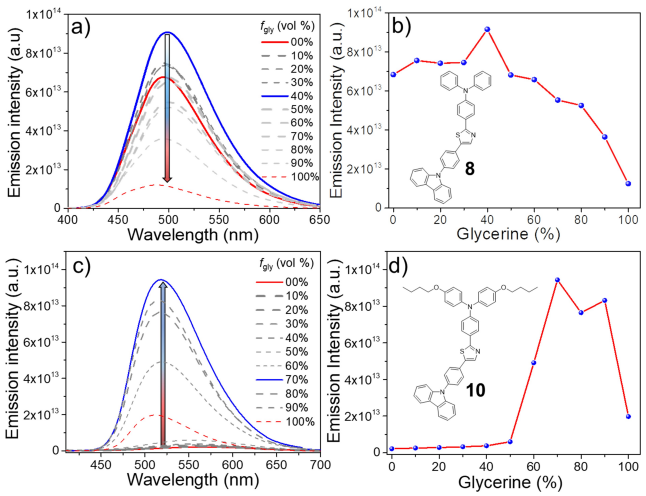

Figure 7. Plots of fluorescence response of **8** (a) and **10** (b) in methanol-glycerol fractions. Plots of glycerol fractions (%) versus emission intensity of **8** (b) and **10** (d).

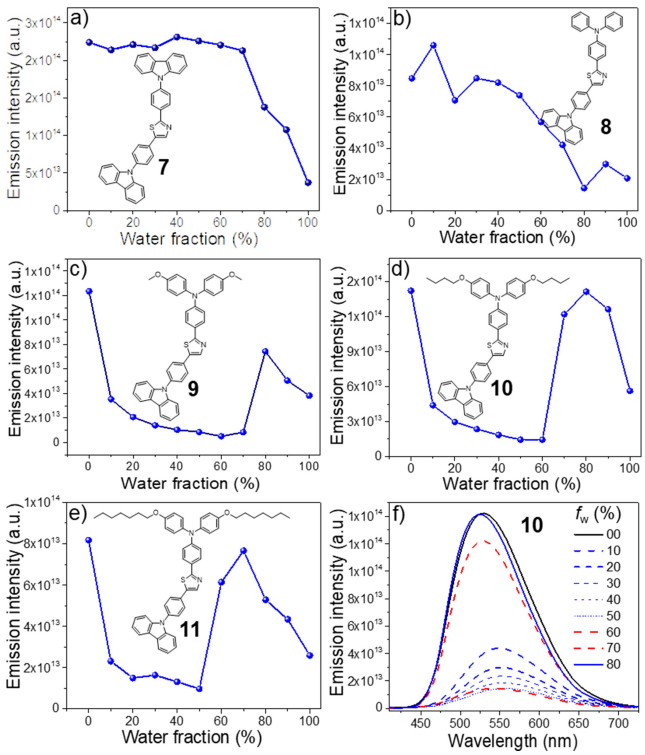

Figure 8. Aggregation experiments for compounds **7** (a), **8** (b), **9** (c), **10** (d,f) and **11** (e) Plot of water fraction (f_w) against emission intensity [4×10^{-3} M].

However, when f_w >60%, the compound experiences less deleterious interactions showing good emission attributed to the appended alkyl chains.

Single crystal X-ray diffraction of compounds 8 and 9

After exploring numerous crystallization conditions, only single crystals of compounds **8**, and **9** were obtained. These crystals grew after a few days by slow evaporation from a mixture of dichloromethane/ethanol. They crystallized as needles or prisms, showing strong fluorescence in green and yellow, respectively (Figure S11). The X-ray data collected at room temperature, the compounds were indexed and solved in either orthorhombic *P*bca and triclinic *P*-1 space group, respectively (CCDC: 2161512 for **8** and 2161513 for **9**) (Table S3). As expected, their molecular structures unveiled torsions among the rings. To provide a better picture of the molecular distortion we calculated the torsion angles between contiguous planes (φ) compiled in Table S4. We observed that the molecules showed torsions with angles as high as 64° (Figure 9a, Figure 9b). Similar molecular distortion was also found in our calculations of isolated systems in solution. This indicates that the molecular electronic structure determines the geometry in the solid-state (Table S4). The overlapped structures revealed a higher distortion in compound **9**, attributed to the *O*-Methyl group (Figure 9c).

The analysis of the crystal packing of **8** showed that molecules were stacked along the a-axis in an antiparallel fashion (Figure S12a). The nitrogen of the thiazole ring sustains a weak hydrogen bond with adjacent phenylene with the CH—N distance d = 2.620 Å and angle of 152.47°. In addition, we observed a parallel displaced π-π interaction d = 3.379 Å between neighboring molecules (Figure S12b). For compound **9** the molecules are arrayed in a staggered motif (Figure S13a). We noted several CH-π interactions, for example between carbazole and a neighboring phenylene with a distance d = 3.517 Å. A weak interaction was also observed between the CH of a thiazole acceptor and one ring of a triphenylamine donor with a distance d = 3.211 Å (Figure S13b).

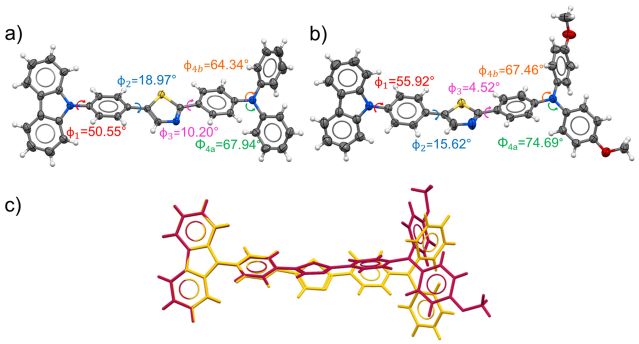

Figure 9. Crystal structure and torsion angles between rings for a) compound **8**, b) compound **9**, and c) overlapped structures to highlight the different molecular conformations.

Solid-state emission of compounds 7–10

After establishing the emissive properties in solution and the structural features from the X-ray data, we set out to characterize the solid-state emission of the compounds. It is relevant to note that compound **11** with the longer aliphatic chains gives rise to a waxy solid that was difficult to crystallize and since it was no longer studied in this section, we focused our efforts on compounds **7**–**10**.

The solid-state emission of compound **7** (λ_{em} = 471 nm) is red-shifted by 31 nm when compared to its fluorescence in solution. A similar redshift is observed for compound **8** (λ_{em} = 502 nm). Similarly, behavior for compounds **9** (λ_{em} = 533 nm) and **10** (λ_{em} = 526 nm) (Figure 10). Regarding the quantum yields in solid, when the synthesis at higher scale was performed, compounds **7** and **8** were obtained as crystalline solids whereas compounds **9** and **10** as amorphous solids (Figure S14–S16). A quantum yield of Φ_{solid} = 0.14 was determined for compound **7**, but when the carbazole fragment is replaced by a diphenylamine group a 4-fold increase is observed (**8**; Φ_{solid} = 0.59). The smaller QY for compound **7** is in line with its larger reorganization energy (λ = 0.49 and 0.39 eV for **7** and **8** in methanol respectively), which may indicate a larger probability of nonradiative decay. The rise in emission could be attributed to the torsion generated by the diphenylamine fragment, which was observed in the X-ray structure above. Conversely, for compounds **9** and **10** moderate values were observed (Φ_{solid} = 0.18 and Φ_{solid} = 0.22), respectively, although higher QY values were expected for the latter compounds, their amorphous nature may account for the discrepancy. It is possible to correlate the observed DSE properties with seminal works of thiazoles, previously mentioned in the introduction section. For instance, the QY values of the fluorophores **7**–**11** reported here are higher than those found in compounds reported by Belskaya,[10] but comparable to or even lower than those found in compounds reported by Murai.[11b,17a]

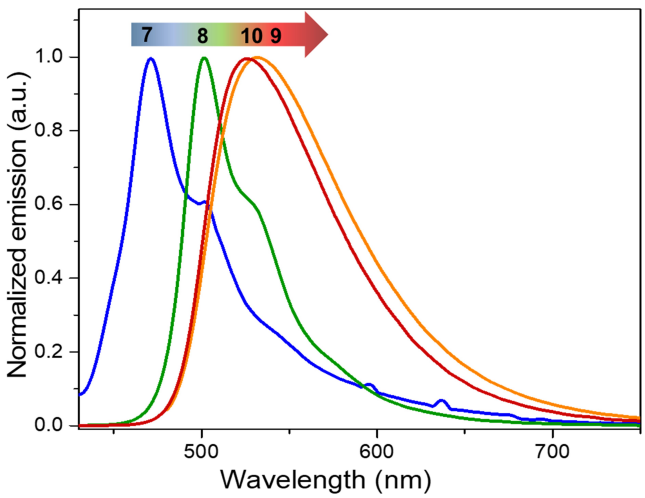

Figure 10. Fluorescence of the thiazole-based derivatives **7**–**10** in solid-state.

Conclusion

Using a three-component, Rh(II) catalyzed reaction; we successfully prepared a new series of D–A–D′ compounds using 2,5-disubstituted thiazoles as the acceptor fragment. The synthesized series showed the Dual-State Emission property with excellent fluorescence in solution (Φ_{THF} = 73–100 %) and moderate solid-state emission (Φ_{solid} = 14–59 %). Furthermore, the aggregation experiments allowed us to understand that including *O*-alkyl substituents facilitates the self-isolation effect, with the best results achieved using four carbon atoms chains (compound **10**). Polarity studies and computational simulations helped us rationalize the effect of the dielectric constant on the emissive response and the role of the charge transfer between the molecular D–A–D′ components. Our systematic approach indicates that a multicomponent synthetic approach can be implemented to develop DSE materials, which could be used in future biological and/or optoelectronic applications.

Experimental section

Crystallographic data

Deposition Numbers 2161512 (for **8**) and 2161513 (for **9**) contain the supplementary crystallographic data for this paper. These data are provided free of charge by the joint Cambridge Crystallographic Data Centre and Fachinformationszentrum Karlsruhe Access Structures service www.ccdc.cam.ac.uk/structures.

Acknowledgements

This project was supported by PAPIIT (IN207222), and CONACYT (A1-S-32820). J.L.B.-V thanks DGAPA of UNAM for a postdoctoral fellowship grant. E. A. H.-M thanks CONACYT for a MSc. Scholarship (1078913). R. C. O and F. J. H acknowledge the Leverhulme Trust (RPG-2019-122) for funding. We utilized Queen Mary's Apocrita HPC facility, supported by QMUL Research-IT. We acknowledge the technical assistance from Dr. R. A. Toscano, Dra. B. Quiroz, Dra. Adriana Romo Pérez, M. A. Peña-González, E. Huerta-Salazar, Dr. Yoarhy A. Amador-Sánchez and Dr. Mario Rodríguez (CIO).

Conflict of Interest

The authors declare no conflict of interest.

Data Availability Statement

The data that support the findings of this study are available from the corresponding author upon reasonable request.

Keywords: Aggregation · Donor–acceptor systems · Dual-state emission · Dyes · Thiazole

[1] a) J. L. Belmonte-Vázquez, Y. A. Amador-Sánchez, L. A. Rodríguez-Cortés, B. Rodríguez-Molina, *Chem. Mater.* **2021**, *33*, 7160–7184; b) L. A. Rodríguez-Cortés, A. Navarro-Huerta, B. Rodríguez-Molina, *Matter.* **2021**, *4*, 2622–2624.
[2] a) J. Zhou, M. Huang, Z. Zhu, Y. Wan, *Chin. Chem. Lett.* **2021**, *32*, 445–448; b) S.-H. Chen, S.-H. Luo, L.-J. Xing, K. Jiang, Y.-P. Huo, Q. Chen, Z.-Y. Wang, *Chem. Eur. J.* **2022**, *28*, e202103478.
[3] J. Mei, N. L. C. Leung, R. T. K. Kwok, J. W. Y. Lam, B. Z. Tang, *Chem. Rev.* **2015**, *115*, 11718–11940.
[4] a) Q. Qiu, P. Xu, Y. Zhu, J. Yu, M. Wei, W. Xi, H. Feng, J. Chen, Z. Qian, *Chem. Eur. J.* **2019**, *25*, 15983–15987; b) Y. Tu, Z. Zhao, J. W. Y. Lam, B. Z. Tang, *Natl. Sci. Rev.* **2021**, *8*, nwaa260; c) Y. Zhang, Y. Qu, J. Wu, Y. Rui, Y. Gao, Y. Wu, *Dyes Pigm.* **2020**, *179*, 108431.
[5] a) Y. Xu, L. Ren, D. Dang, Y. Zhi, X. Wang, L. Meng, *Chem. – Eur. J.* **2018**, *24*, 10383–10389; b) F. Yu, H. Zhao, Y. Li, G. Xia, H. Wang, *Mater. Chem. Front.* **2022**, *6*, 155.
[6] a) Y. Zhang, Y. Qu, J. Wu, Y. Rui, Y. Gao, Y. Wu, *Dyes Pigm.* **2020**, *179*, 108431; b) Y. Xu, L. Ren, D. Dang, Y. Zhi, X. Wang, L. Meng, *Chem. Eur. J.* **2018**, *24*, 10383–10389; c) S. Qu, Q. Lu, S. Wu, L. Wang, X. Liu, *J. Mater. Chem.* **2012**, *22*, 24605–24609.
[7] X. Song, M. Wang, L. Kong, J. Zhao, *RSC Adv.* **2017**, *7*, 18189–18198.
[8] a) S. Achelle, N. Plé, *Curr. Org. Synth.* **2012**, *9*, 163–187; b) Y. Wu, W. Zhu, *Chem. Soc. Rev.* **2013**, *42*, 2039; c) N. A. Kukhta, M. R. Bryce, *Mater. Horiz.* **2021**, *8*, 33.
[9] T. Tao, B.-B. Ma, Y.-X. Peng, X.-X. Wang, W. Huang, X.-Z. You, *J. Org. Chem.* **2013**, *78*, 8669–8679.
[10] P. O. Suntsova, A. K. Eltyshev, T. A. Pospelova, P. A. Slepukhin, E. Benassi, N. P. Belskaya, *Dyes Pigm.* **2019**, *166*, 60–71.
[11] a) K. K. P. Pamungkas, T. Maruyama, T. Murai, *Org. Biomol. Chem.* **2021**, *19*, 6804; b) Y. Tsuchiya, K. Yamaguchi, Y. Miwa, S. Kutsumizu, M. Minoura, T. Murai, *Bull. Chem. Soc. Jpn.* **2020**, *93*, 927–935.
[12] K. Godugu, R. T. Gundala, R. Bodapati, V. D. S. Yadala, S. S. Loka, C. G. R. Nallagondu, *New J. Chem.* **2020**, *44*, 7007.
[13] K. l. Lugovic, A. V. Popova, A. K. Eltyshev, E. Benassi, N. P. Belskaya, *Eur. J. Org. Chem.* **2017**, 4175–4187.
[14] K. Godugu, S. Shaik, M. K. M. Pinjari, T. R. Gundala, D. V. C. Subramanyam, S. S. Loka, H. Divi, V. Venkatramu, G. R. Nallagondu, *Dyes Pigm.* **2021**, *187*, 109077.
[15] a) A. Mishra, M. K. R. Fischer, P. Bäuerle, *Angew. Chem. Int. Ed.* **2009**, *48*, 2474–2499; *Angew. Chem.* **2009**, *121*, 2510–2536; b) I. Bulut, P. Chávez, A. Mirloup, Q. Huaulmé, A. Hébraud, B. Heinrich, S. Fall, S. Méry, R. Ziessel, T. Heiser, P. Lévêque, N. Leclerc, *J. Mater. Chem. C.* **2016**, *4*, 4296.
[16] Y. Lin, H. Fan, Y. Li, X. Zhan, *Adv. Mater.* **2012**, *24*, 3087–3106.
[17] a) T. Murai, M. Yoshihara, K. Yamaguchi, M. Minoura, *Asian J. Org. Chem.* **2019**, *8*, 1102–1106; b) T. Murai, K. Yamaguchi, T. Hayano, T. Maruyama, K. Kawai, H. Kawakami, A. Yashita, *Organometallics* **2017**, *36*, 2552–2558; c) M. R. Shreykar, N. Sekar, *Dyes Pigm.* **2017**, *142*, 121–125; d) R. P. Tayade, N. Sekar, *J. Fluoresc.* **2017**, *27*, 167–180; e) K. Atippich, D. Weiss, A. Guether, H. Gorls, R. Beckert, *J. Sulfur Chem.* **2009**, *30*, 109–118.
[18] a) A. Helal, N. T. T. Thao, S. W. Lee, H.-S. Kim, *J. Inclusion Phenom. Macrocyclic Chem.* **2010**, *66*, 87–94; b) R. Menzel, D. Ogermann, S. Kupfer, D. Weiß, H. Görls, K. Kleinermanns, L. González, R. Beckert, *Dyes Pigm.* **2012**, *94*, 512–524; c) M.-Y. Yang, X.-L. Zhao, M.-H. Zheng, Y. Wang, J.-Y. Jin, *J. Fluoresc.* **2016**, *26*, 1653–1657; d) Z. Sahin, M. Ertas, B. Berk, S. N. Biltekin, L. Yurttas, S. Demirayak, *Bioorg. Med. Chem.* **2018**, *26*, 1986–1995.
[19] B. Xi, N. Wang, B.-B. Ma, T. Tao, W. Huang, *Tetrahedron.* **2015**, *71*, 3966–3975.
[20] a) H. Wu, Z. Chen, W. Chi, A. K. Bindra, L. Gu, C. Qian, B. Wu, B. Yue, G. Liu, G. Yang, L. Zhu, Y. Zhao, *Angew. Chem. Int. Ed.* **2019**, *58*, 11419–11423; *Angew. Chem.* **2019**, *131*, 11541–11545; b) Y. Wang, W. Liu, L. Bu, J. Li, M. Zheng, D. Zhang, M. Sun, Y. Tao, S. Xue, W. Yang, *J. Mater. Chem. C* **2013**, *1*, 856.
[21] a) S. Chakraborty, K. Harris, M. Huang, *AIP Adv.* **2016**, *6*, 12513; b) A. Shundo, Y. Okada, F. Ito, K. Tanaka, *Macromolecules* **2012**, *45*, 329–335; c) P. Minei, A. Battisti, S. Barondi, M. Lessi, F. Bellina, G. Ruggeri, A. Pucci, *ACS Macro Lett.* **2013**, *4*, 317–321.
[22] a) S. Tani, T. N. Uehara, J. Yamaguchi, K. Itami, *Chem. Sci.* **2014**, *5*, 123–135; b) X.-W. Liu, J.-L. Shi, J.-X. Yan, J.-B. Wei, K. Peng, L. Dai, C.-G. Li, B.-Q. Wang, Z.-J. Shi, *Org. Lett.* **2013**, *22*, 5774–5777; c) *C–H Activation—Topics in Current Chemistry* (Eds: J.-Q. Yu, Z. Shi), Springer, Berlin, **2010**.
[23] a) A. K. Eltyshev, T. H. Dzhumaniyazov, P. O. Suntsova, A. S. Minin, V. A. Pozdina, W. Dehaen, E. Benassi, N. P. Belskaya, *Dyes Pigm.* **2021**, *184*, 108836; b) N. P. Belskaya, I. Kostova, Z. Fan, *Targets Heterocycl. Syst.* **2020**, *23*, 116–142.

Research Article
doi.org/10.1002/ejoc.202200372

[24] T. Miura, Y. Funakoshi, Y. Fujimoto, J. Nakahashi, M. Murakami, *Org. Lett.* **2015**, *17*, 2454–2457.
[25] A. Aguilar-Granda, S. Pérez-Estrada, A. E. Roa, J. Rodríguez-Hernández, S. Hernández-Ortega, M. Rodríguez, B. Rodríguez-Molina, *Cryst. Growth Des.* **2016**, *16*, 3435–3442.
[26] a) Y. Matsumoto, T. Tsuji, D. Nakatake, R. Yazaki, T. Ohshima, *Asian J. Org. Chem.* **2019**, *8*, 1071–1074; b) D. Cho, J. Ahn, K. A. De Castro, H. Ahn, H. Rhee, *Tetrahedron* **2010**, *66*, 5583–5588.
[27] E. Zaborova, P. Chávez, R. Bechara, P. Lévêque, T. Heiser, S. Méry, N. Leclerc, *Chem. Commun.* **2013**, *49*, 9938.
[28] N. L. C. Leung, N. Xie, W. Yuan, Y. Liu, Q. Wu, Q. Peng, Q. Miao, J. W. Y. Lam, B. Z. Tang, *Chem. Eur. J.* **2014**, *20*, 15349–15353.
[29] H. Wu, Z. Chen, W. Chi, A. K. Bindra, L. Gu, C. Qian, B. Wu, B. Yue, G. Liu, G. Yang, L. Zhu, Y. Zhao, *Angew. Chem.* **2019**, *131*, 11541–11545.

Manuscript received: March 30, 2022
Revised manuscript received: May 16, 2022
Accepted manuscript online: May 21, 2022

RESEARCH ARTICLE

In this work, a new series of thiazole-based dual-state emission fluorophores with self-isolation properties in solution and good emission in the solid state are reported.

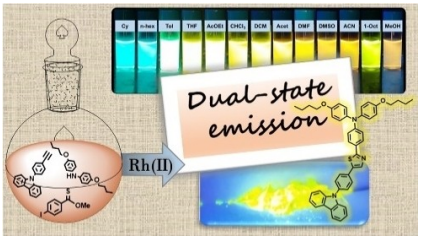

Dr. J. L. Belmonte-Vázquez, BSc. E. A. Hernández-Morales, Dr. F. Hernández, Dr. M. C. García-González, Dr. L. D. Miranda, Dr. R. Crespo-Otero, Dr. B. Rodríguez-Molina**

1 – 9

Asymmetric Dual-State Emitters Featuring Thiazole Acceptors